

pH-Dependent UV Resonance Raman Spectra of Cytosine and Uracil

Brant E. Billinghamurst, Sulayman A. Oladepo, and Glen R. Loppnow*

Department of Chemistry, University of Alberta, Edmonton, Alberta T6G 2G2, Canada

Received: December 22, 2008; Revised Manuscript Received: March 20, 2009

Cytosine is a nucleobase found in both DNA and RNA, while uracil is found only in RNA. Uracil has abstractable protons at N₃ and N₁. Cytosine has only one abstractable proton at N₁ but can also accept a proton at N₃. The pK_a values of these protons are well-known, but the effect of the change in protonation on the rest of the molecule is not well understood and is very important in base stacking, base pairing, and protein–nucleic acid interactions. In this paper, UV resonance Raman (UVR) spectroscopy is used to probe the structures of both cytosine and uracil at varying pH to determine the structural changes that take place. The results show that cytosine has increased electronic delocalization when moving to either basic or acidic environments, whereas uracil shows no significant change in acidic environment but increases its electronic delocalization in basic environment.

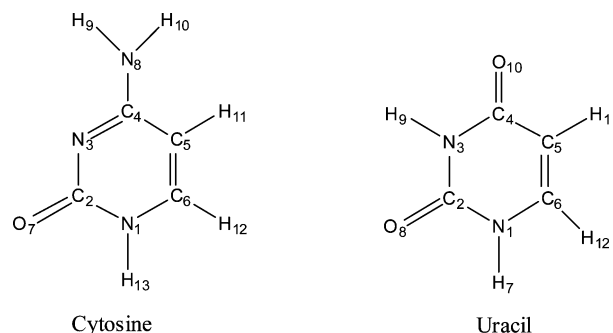
Introduction

Cytosine (4-amino-2-oxypyrimidine) is one of the four nucleobases found in DNA and RNA, while uracil (2,4-dioxypyrimidine) is only found in RNA¹ (Scheme 1). In nearly all of the base pairing structures which involve cytosine or uracil, N₃ has a major role.² If N₃ is protonated, it can interact by hydrogen bonding with a carbonyl or another unprotonated nitrogen. If not protonated, it may interact with protons on the other base. Furthermore, the carbonyls are also very important in base pairing, and any changes in the electronic delocalization that affects the carbonyls will have ramifications on this hydrogen bonding interaction. To understand fully the nature of base-paired nucleobases, probes of the electronic structure of the nucleobases are needed.

Changes in the absorption spectra of nucleobases with varying pH have been observed as early as 1945.³ The unstacking of thymine and cytosine as a function of pH on DNA has been observed previously with Raman spectroscopy,⁴ although difference spectra were used due to the complexity of the spectra. Using difference spectra is less reliable, as small changes between spectra that may not be due to the changes in the sample may be magnified.⁴ Evidence of increased electronic delocalization in uracil at high pH has been found using coherent anti-Stokes Raman scattering (CARS), but this study was limited to only the 850–1247 cm⁻¹ region of the spectra.⁵

Raman spectroscopy is a powerful probe of structure and interactions of nucleobases.^{6–12} It is particularly useful for a study of the effect of pH in aqueous solutions, since water has a very small Raman signal that does not interfere with the signal from the nucleobases. In contrast, proton NMR and IR studies would require the use of deuterated or nonaqueous solvents which are less biologically relevant and expensive. Ultraviolet resonance Raman (UVR) spectroscopy also offers the added advantage over Raman spectroscopy of resonance enhancement, allowing lower concentrations to be used. This advantage is particularly useful in the case of cytosine and uracil, as both have relatively low solubility in water. Finally, resonant enhancement occurs for those vibrational modes that are coupled

SCHEME 1



to the electronic excitation.¹² Therefore, UVR spectroscopy is also sensitive to the electronic structure in both the ground and excited states.

In this work, we examine the effect of pH on the UVR spectra of cytosine and uracil. Although a number of researchers have examined the UVR spectra of the nucleic acids and their components,^{7–11} none have probed electronic structure changes as a function of pH. The resulting spectra do indeed change as a function of increasing pH, reflecting the deprotonation of various functional groups in the pyrimidine nucleobases. The most evident effect of pH changes for cytosine and uracil is protonation/deprotonation of N₃, which have pK_a's of 4.6 and 9.5, respectively.^{13,14} The pK_a's of the N₁ protons are 12.2 and > 13 for cytosine and uracil, respectively.^{13,14} The results of the experiments reported here are discussed within a model of electronic structure change as a function of pH.

Experimental Section

Cytosine (4-amino-2-oxypyrimidine, 99%) and uracil (2,4-dioxypyrimidine, 99%) were purchased from Sigma (Oakville, Ontario), sodium hydroxide (97%) was purchased from BDH Inc. (Toronto, Ontario), and hydrochloric acid was purchased from Anachemia (Montreal, Quebec) and Caledon Laboratories Ltd. (Georgetown, Ontario). All chemicals were used without further purification. All samples were prepared using nanopure water from a Barnstead (Dubuque, Iowa) water filtration system.

* To whom correspondence should be addressed. E-mail: glen.loppnow@ualberta.ca. Phone: 780-492-9704. Fax: 780-492-8231.

Laser excitation for the resonance Raman experiments was obtained from a Coherent (Santa Clara, CA) picosecond mode-locked Ti:sapphire laser pumped with a doubled, solid-state, diode-pumped continuous wave Nd:YAG laser. In order to obtain 257 and 285 nm, the output of the Ti:sapphire laser was doubled using a lithium triborate (LBO) crystal followed by third harmonic generation in a β -barium borate (β -BBO) crystal in an Inrad (Northvale, NJ) harmonic generator. Typical UV laser powers were 6–20 mW at the sample. The resulting laser beam was spherically focused on an open stream of flowing solution in a 135° backscattering geometry. The resonance Raman scattering was focused into a double-grating spectrometer with a diode array detector. The laser system and spectrometer have been described in detail previously.^{7,8} For each spectrum, the total accumulation time was 5–15 min.

The collection of spectra was done in four sets of experiments for cytosine and uracil, each beginning with 100 mL of 0.018 M cytosine or uracil solution. In order to collect spectra from pH values of ~ 7 to ~ 0.5 , the cytosine solution was titrated with either 0.02 or 2 M HCl solutions and spectra were collected every ca. 0.5 pH units. This titration was repeated twice, once to collect spectra in the $550\text{--}1400\text{ cm}^{-1}$ range and once to collect spectra in the $1050\text{--}1800\text{ cm}^{-1}$ range. The same process was repeated, in order to collect spectra for pH values of ~ 7 to ~ 13.5 , but titrating with 0.02 or 2 M NaOH solutions. For all spectra, the water spectrum was subtracted and the baseline was leveled and zeroed. For the uracil resonance Raman spectra at high pH, 0.4 M sodium sulfate was also added; it had no effect on the absorption or resonance Raman spectrum of uracil. Frequency calibration was performed by measuring the Raman scattering of solvents for which the peak positions are known (*n*-pentane, cyclohexane, *N,N*-dimethylformamide, ethanol, acetonitrile, and acetic acid). Frequencies are accurate to $\pm 2\text{ cm}^{-1}$.

Absorbance spectra were collected with a Hewlett-Packard (Palo Alto, California) HP 8452A diode array spectrophotometer for 0.09 mM uracil and cytosine at various pH values using a 1 cm path length cuvette. The required pH values were obtained by adding to the 0.09 mM uracil solution either 0.02 or 2 M HCl or NaOH solution. These acid and base solutions also contained 0.09 mM uracil to avoid dilution of the sample as the pH adjustment progressed. The pH values varied within ± 0.03 pH units.

Results

Absorption spectra of cytosine and uracil at various pH values are shown in Figure 1. The 266 nm absorbance band of cytosine at pH 5.6 shifts to 282 nm at pH 13.2 and to 276 nm at pH 1 (Figure 1). For uracil, the 260 nm absorption band at pH 5.6 decreases as the pH is raised and a new band appears at higher wavelength, ca. 290 nm (Figure 1). For uracil, there was no change in the absorption spectrum as the pH was lowered.

The UVRR spectra of cytosine and uracil in water at 257 nm are shown in Figure 2. Assignments based on the DFT and MP2 calculations done by Gaigeot et al.¹⁵ are shown in Table 1 for cytosine, and assignments based on a DFT calculation done using the B3LYP/6-311G(d,p) basis set by Yarasi and Loppnow¹⁶ are given in Table 2 for uracil. For this paper, we have concentrated on the $650\text{--}1800\text{ cm}^{-1}$ fingerprint region of the spectrum, as it contains the modes that are of primary interest to this work.

Spectra of the $530\text{--}1450$ and $1050\text{--}1800\text{ cm}^{-1}$ regions of cytosine in solutions of varying pH are shown in Figures 3 and 4, respectively. There are a number of peaks that are affected by the changes in pH in cytosine. In the following paragraphs,

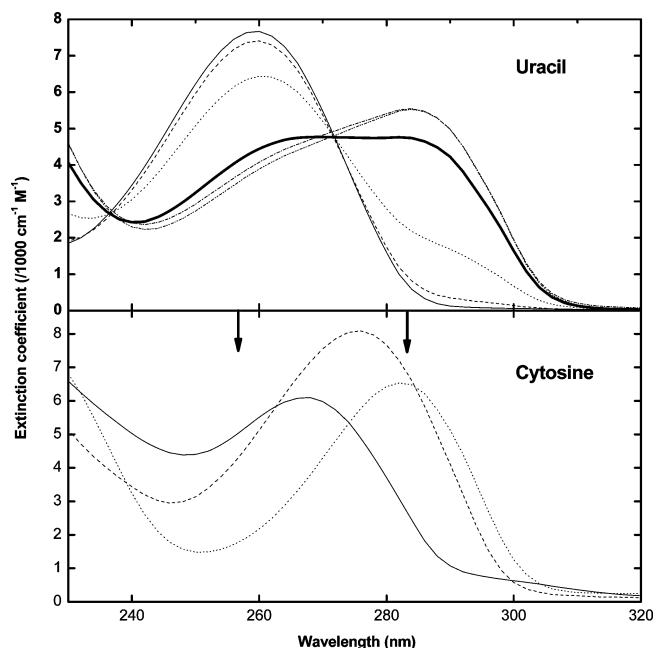


Figure 1. (top) Absorption spectra of uracil (0.09 mM) at pH values of 5.6 (solid), 8 (dash), 9 (dot), 10 (bold solid), 11 (dash-dot), and 12 (dash-dot-dot). (bottom) Absorption spectra of 0.09 mM cytosine at pH 1.0 (dash), 5.6 (solid), and 13.2 (dot). The arrows indicate the UV resonance Raman excitation wavelengths.

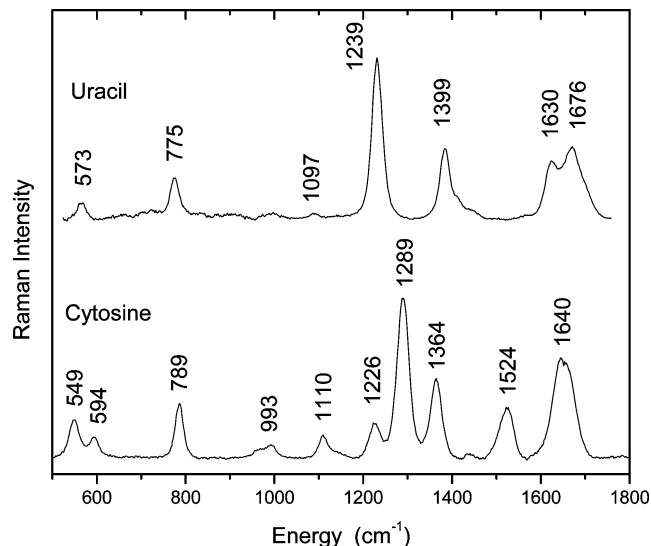


Figure 2. UV resonance Raman spectrum of 0.018 M uracil (top) and cytosine (bottom) in water (pH ~ 7) and excited at 257 nm.

peaks will be identified by their frequency in water. As cytosine is titrated from a pH of 7 to 0.3, all of the significant changes to the spectrum begin to emerge at pH ~ 5 . The intense 1289 cm^{-1} peak shifts to lower frequency to 1272 cm^{-1} at pH 4.5. Weaker peaks at 1110, 1369, and 1524 cm^{-1} peaks all increase in frequency until pH 3.5, settling at 1130, 1384, and 1584 cm^{-1} , respectively. Finally, one of the two overlapping modes that makes up the band at 1640 cm^{-1} shifts to 1730 cm^{-1} . As the cytosine is titrated with base, no significant change is observed until pH ~ 13 is reached. At this pH, the 594 cm^{-1} band shifts to 618 cm^{-1} . The peaks at 1289 and 1640 cm^{-1} lose most or all of their intensity compared to the 789 cm^{-1} band, and new bands appear at 1466 and 1554 cm^{-1} .

The UV resonance Raman spectra of uracil at various pH values in the $650\text{--}1330$ and $1150\text{--}1760\text{ cm}^{-1}$ regions are

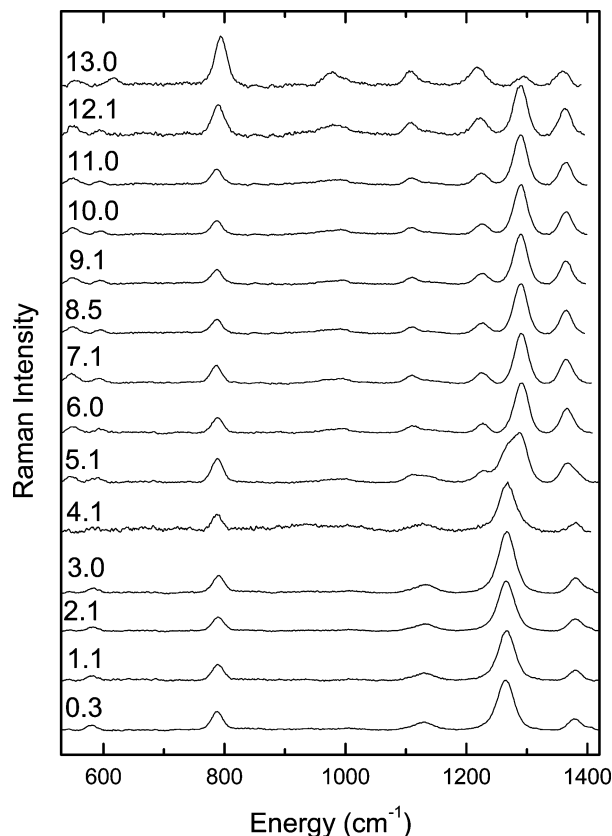


Figure 3. UV resonance Raman spectra (500–1450 cm^{-1}) of cytosine at various pH values excited at 257 nm. For ease of presentation, the spectra have been normalized to the peak with maximum intensity.

TABLE 1: Resonance Raman Vibrational Assignments for Cytosine^a

mode (cm^{-1})	mode assignment ^b
549	$\tau(\text{C}_4\text{--N}_8)$ [17], $\text{be}(\text{N}_1\text{C}_2\text{O}_7)$ [12]
594	$\tau(\text{C}_4\text{--N}_8)$ [17], $\text{be}(\text{N}_3\text{C}_4\text{C}_5)$ [16]
789	$\delta(\text{C}_2\text{=O}_7)$ [74], $\delta(\text{C}_4\text{--N}_8)$ [8]
993	$\delta(\text{C}_6\text{--H}_{12})$ [61], $\tau(\text{C}_5\text{=C}_6)$ [21]
1110	$\text{be}(\text{C}_4\text{N}_8\text{H}_9)$ [50], $\nu(\text{N}_1\text{--C}_6)$ [9]
1226	$\text{be}(\text{N}_1\text{C}_6\text{H}_{12})$ [19], $\nu(\text{N}_1\text{--C}_6)$ [18]
1289	$\nu(\text{C}_2\text{--N}_3)$ [38], $\nu(\text{C}_4\text{--N}_8)$ [13]
1369	$\nu(\text{C}_4\text{--N}_8)$ [18], $\text{be}(\text{C}_5\text{C}_6\text{H}_{12})$ [17]
1524	$\nu(\text{C}_4\text{--N}_8)$ [17], $\nu(\text{N}_3\text{=C}_4)$ [14]
1640	$\nu(\text{C}_5\text{=C}_6)$ [32], $\nu(\text{N}_3\text{=C}_4)$ [13], $\nu(\text{C}_2\text{=O}_7)$ [76]

^aFrequencies listed are the experimental frequencies reported here. ^bAbbreviations: ν is stretching, δ is deformation, be is bending, and τ is torsion. Assignments are from ref 15. Numbers in square brackets represent the percentage potential energy distribution (PED) of the listed internal coordinate(s) to the normal mode. Only the two most significant internal coordinates are listed.

shown in Figures 5 and 6, respectively. There are a number of peaks that are affected by the changes in pH. No significant changes to the uracil spectra are observed as the pH is lowered from 9 to 1.1, consistent with the absorption spectrum and in contrast to what was observed for cytosine. However, the resonance Raman spectrum undergoes a transition between pH 9 and pH 13.

Between pH 9 and 10.5, the 789 cm^{-1} band shifts to 797 cm^{-1} and the weak 1097 cm^{-1} peak shifts to 1105 cm^{-1} and gains intensity. The 1239, 1388, and 1676 cm^{-1} peaks all lose intensity at pH 9, and they are reduced to nothing by pH 11. New peaks appear at 1189, 1290, 1370, 1473, and 1567 cm^{-1} . The 1630 cm^{-1} peak appears to shift to 1640 cm^{-1} and gain intensity from pH 9 to 11.

TABLE 2: Resonance Raman Vibrational Assignments for Uracil^a

mode (cm^{-1})	mode assignment ^b
789	$\nu(\text{C}_4\text{C}_5)$ [28], $\nu(\text{N}_1\text{C}_2)$ [19], ring def 1 [−13], $\nu(\text{N}_3\text{C}_4)$ [10], ring def 3 [−7], $\nu(\text{C}_2\text{N}_3)$ [6], $\nu(\text{C}_6\text{N}_1)$ [6]
1097	$\nu(\text{C}_6\text{N}_1)$ [33], $\text{be}(\text{C}_5\text{H}_{11})$ [23], $\nu(\text{C}_5\text{C}_6)$ [9], $\nu(\text{N}_3\text{C}_4)$ [−9], $\nu(\text{N}_1\text{C}_2)$ [−6]
1239	$\text{be}(\text{C}_5\text{H}_{11})$ [33], $\text{be}(\text{C}_6\text{H}_{12})$ [18], $\nu(\text{C}_6\text{N}_1)$ [−15], $\text{be}(\text{N}_1\text{H}_7)$ [10], $\nu(\text{N}_3\text{C}_4)$ [7], $\nu(\text{N}_1\text{C}_2)$ [5]
1388	$\nu(\text{C}_2\text{N}_3)$ [18], $\text{be}(\text{N}_3\text{H}_9)$ [17], $\nu(\text{N}_1\text{C}_2)$ [−15], $\text{be}(\text{C}_5\text{H}_{11})$ [13], $\text{be}(\text{C}_6\text{H}_{12})$ [−12], $\nu(\text{C}_5\text{C}_6)$ [−8], $\text{be}(\text{C}_4\text{O}_{10})$ [5]
1630	$\nu(\text{C}_5\text{C}_6)$ [61], $\text{be}(\text{C}_6\text{H}_{12})$ [−14], $\nu(\text{C}_6\text{N}_1)$ [−8]
1676	$\nu(\text{C}_4\text{O})$ [71], $\nu(\text{C}_4\text{C}_5)$ [−8], ring def 2 [5]

^aFrequencies listed are the experimental frequencies reported here. ^bAbbreviations: ν is stretching, def is deformation, and be is bending. Assignments are from ref 16. Numbers in square brackets represent the percentage potential energy distribution (PED) of the listed internal coordinate(s) to the normal mode.

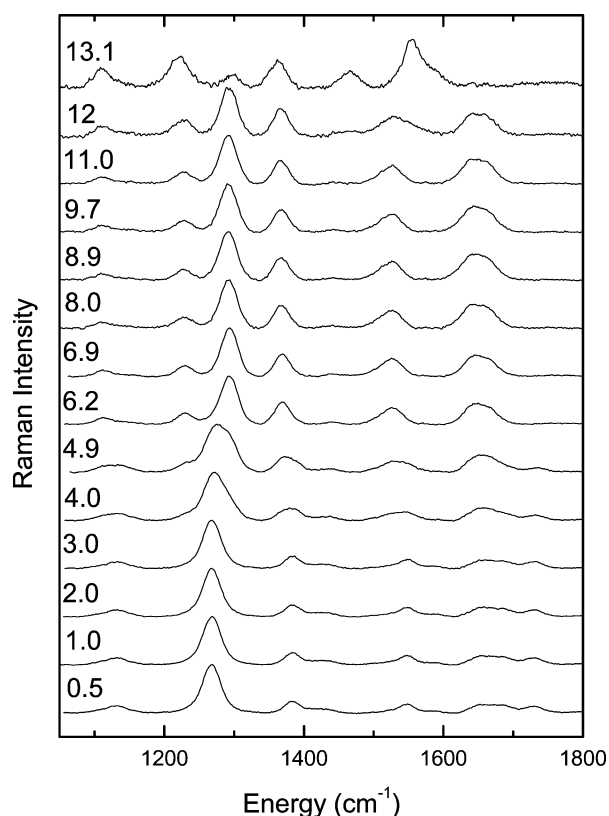


Figure 4. UV resonance Raman spectra of cytosine as per Figure 3 but in the 1050–1800 cm^{-1} region.

Figure 7 shows the UV resonance Raman spectra of uracil at high pH values, excited at 285 nm. Excitation at this wavelength enhances the high pH form of uracil via its 282 nm absorption band. The spectrum obtained is very similar to the visible-excited Raman spectrum of the high pH form of thymine reported earlier,¹⁷ suggesting that the changes to the resonance Raman spectrum observed here are due to ground-state changes in electronic structure, rather than excited-state structural changes. In particular, the new modes observed at 800, 1150, and 1200 cm^{-1} are also seen in the high pH Raman spectrum of thymine.¹⁷ We are currently using computational techniques to explore the ground-state structure of the pyrimidine nucleobases in their various protonation states.

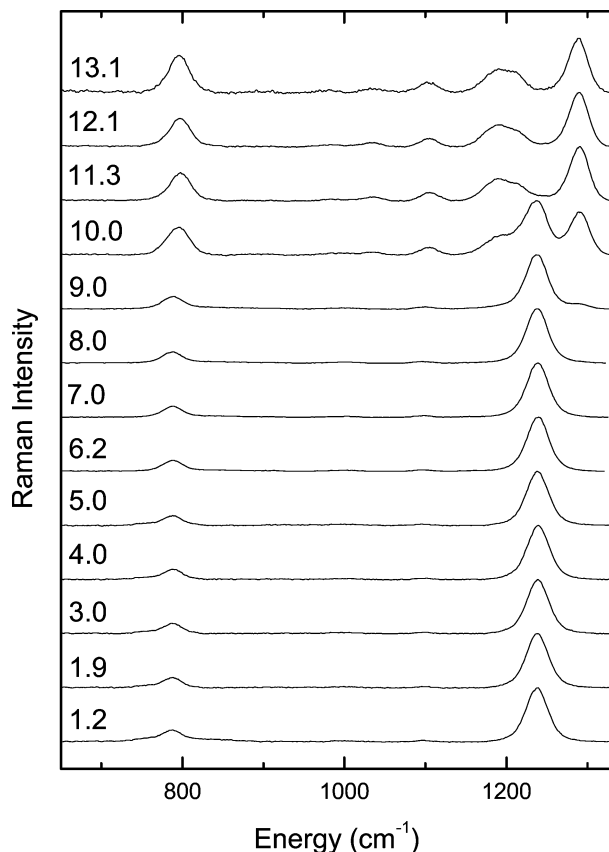


Figure 5. UV resonance Raman spectra (650–1330 cm^{-1}) of uracil (concentrations vary) at various pH values excited at 257 nm. For ease of presentation, the spectra have been normalized to the peak with maximum intensity.

Discussion

Changes in pH reflect the structural changes involved in nucleobase base pairing within DNA and may cause large changes in the electronic structure and delocalization within the molecule, which we will be considering here. UVRR spectroscopy offers significant insight into electronic delocalization, since the frequency of each band is directly related to the bond strength between the atoms involved. Intensity changes can also give insight into changes in coupling or electronic structure. In the following discussion, all of the observed changes in the UVRR spectra will be used to develop a model of the protonated/deprotonated structures of uracil and cytosine. Though a large number of resonance and zwitterionic structures are possible, only the most prevalent will be considered.

For the sake of clarity, the UVRR changes for cytosine that occur between pH 7 and 0 and between pH 7 and 14 will be discussed separately. Looking at the spectra between pH 7 and 0, the most drastic change observed is the shift of the 1289 cm^{-1} band to 1268 cm^{-1} . The fact that the band reaches its lowest energy at pH ~ 4.2 coincides with the pK_a of the N_3 proton.^{13,14} This shift in this peak suggests that it reflects the protonation state of N_3 . That the 1289 cm^{-1} band is assigned to $\nu(\text{C}_2\text{--N}_3)$ [38], $\nu(\text{C}_4\text{--N}_8)$ [13], is consistent with the increased mass at N_3 (Scheme 1) and a weakening of the $\text{C}_2\text{--N}_3$ bond due to the proton withdrawing electron density. A new band at 1710 cm^{-1} could be the $\text{N}\text{--H}$ bend on a $\text{--C=N}^+\text{H}$ moiety.¹⁸ While this shift in the 1289 cm^{-1} band is fairly easy to explain, shifts to higher energy of both the 1364 cm^{-1} band and a component of the 1640 cm^{-1} band are not so straightforward. The 1364 cm^{-1} band and the component of the 1640 cm^{-1} band

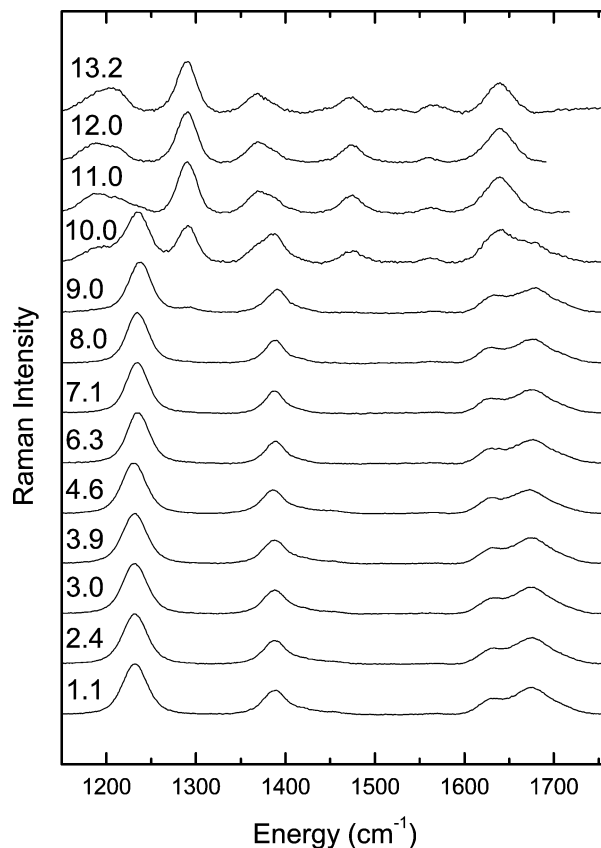


Figure 6. UV resonance Raman spectra (1150–1760 cm^{-1}) of uracil (concentrations vary) at various pH values excited at 257 nm. For ease of presentation, the spectra have been normalized to the peak with maximum intensity.

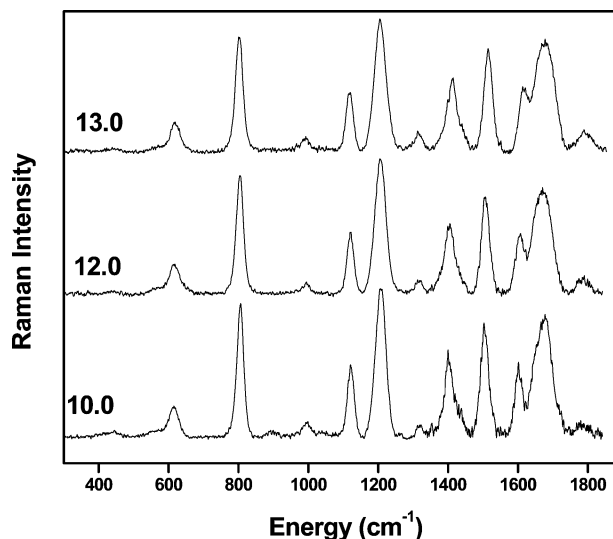
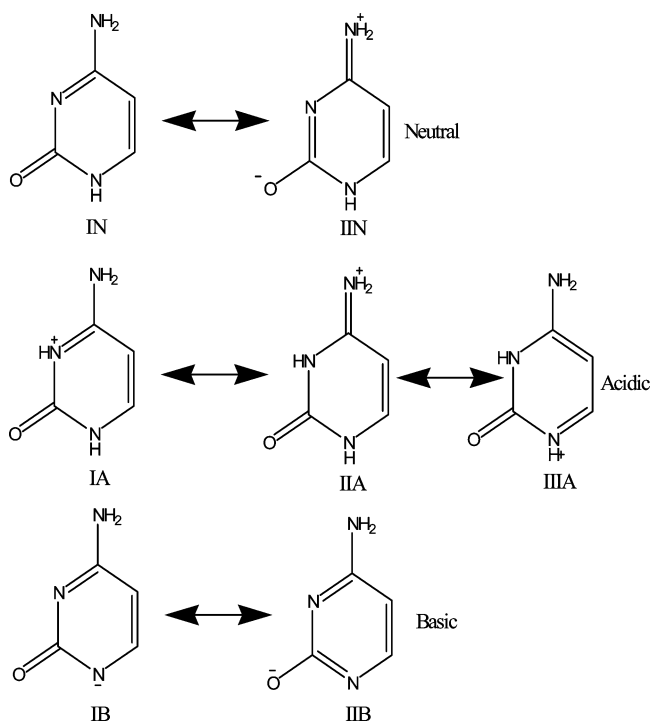


Figure 7. UV resonance Raman spectra of uracil at various pH values excited at 285 nm. For ease of presentation, the spectra have been normalized to the peak with maximum intensity.

in question are assigned to the $\nu(\text{C}_4\text{--N}_8) + \text{be}(\text{C}_5\text{C}_6\text{H}_{12})$ mode and to the $\nu(\text{C}_2\text{=O}_7)$ mode, respectively. These shifts suggest that both the $\text{C}_4\text{--N}_8$ and $\text{C}_2\text{=O}_7$ bonds become stronger under acidic conditions. To explain these observations, the possible delocalization of electron density in cytosine must be considered. To explain the increase in the $\text{C}_2\text{=O}_7$ frequency, an increase of the bond order is likely, suggesting that the delocalization of the lone pair electrons on N_3 to the $\text{C}_2\text{--N}_3$ bond present in neutral solutions is lacking in acidic solutions after protonation

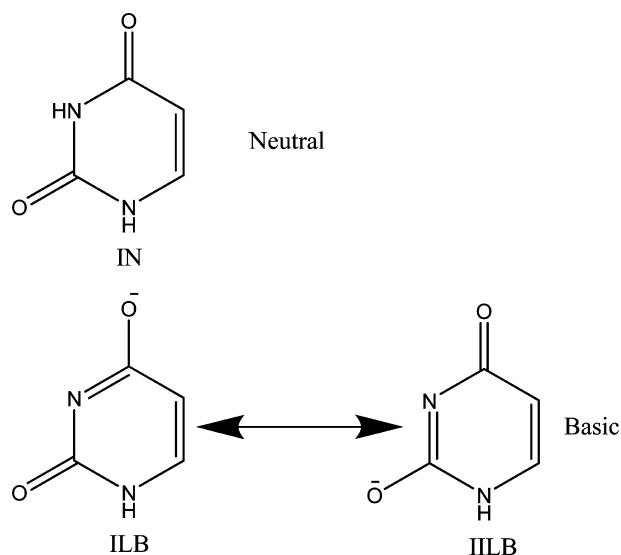
SCHEME 2



of N_3 (see Scheme 2). The shift observed for the $\nu(C_4-N_8)$ vibration (1524 cm^{-1}) may be explained by an increase in the double bond character of the C_4-N_8 bond. Note that, in Scheme 2, both the neutral and acidic schemes have the C_4-N_8 bond with some double bond character. The results suggest that the resonance structure IIA predominates in acid. An increase in the double bond character of the C_4-N_8 bond also explains the shift of the 1110 cm^{-1} band, which involves the $C_4N_8H_9$ bend. The change in the intensity of the 549 cm^{-1} band, combined with the lack of change for the 594 cm^{-1} band, is difficult to explain, as they both involve the C_4-N_8 torsion. However, for both of these vibrations, the available PED only describes 30% of the mode; these vibrations are very delocalized. This model is supported by the observed shift in the absorption spectrum (see Figure 1) from 266 nm at pH 5.6 to 276 nm at pH 1; a longer conjugation that is created by the addition of the proton (Scheme 2) leads to a longer wavelength absorption band.

In basic solution, the UVR spectrum of cytosine changes little until pH 13.1, at which point several sudden changes are observed. Perhaps the most dramatic are the almost complete loss of intensity of the 1289 and 1640 cm^{-1} bands. These bands are attributed to the stretching of the C_2-N_3 and $C_4=C_5$ bonds and of the $C_2=O_7$ bond, respectively. This result could be explained by deprotonation at N_1 , leading to a structure with the electrons delocalized over the entire ring (IIB, Scheme 2). In this type of structure, we would expect both the 1289 cm^{-1} peak and the $C_4=C_5\text{ cm}^{-1}$ component of the 1640 cm^{-1} peak to disappear. Furthermore, new ring stretching bands would be expected to appear, such as the peak observed at 1466 cm^{-1} . The loss of the $C_2=O_7$ component of the 1640 cm^{-1} peak is likely due to the lack of $C_2=O_7$ double bond character in the predominant resonance structure, leading to a new peak at lower frequency, 1554 cm^{-1} . This increased delocalization at high pH is also consistent with the observed shift in the absorption spectrum (Figure 1), where the 266 nm peak that is seen at pH 5.6 shifts to 282 nm at pH 13.2. Again, the suggested structural change leads to a greater delocalization of the electrons over a longer distance, with a consequently longer wavelength absorption.

SCHEME 3



For uracil, no spectral changes are observed at pH values below 9, suggesting that uracil does not undergo protonation above a pH of 1. As uracil is titrated with base, however, many changes are observed. Table 2 shows that, with the exception of the 1640 and 1676 cm^{-1} vibrations, all vibrations have at least some degree of a ring stretching or bending mode in them. As for cytosine, it is likely that the abstraction of a proton will cause large changes to the electron delocalization in the ring. Unfortunately, since most of the modes do in fact involve a ring mode and most of the new peaks that appear are also likely associated with ring modes, it is very difficult to assign the changes to the spectrum directly to specific structural changes. Since most of the changes that are observed start to appear around pH 9, near the 9.5 pK_a value of the N_3 proton, this is the most likely site of deprotonation. The expected resonance structures for neutral and basic pH are illustrated in Scheme 3. The two basic resonance structures would explain the shift of the 789 cm^{-1} peak upon deprotonation of N_3 , as the N_3H deformation would no longer contribute to this mode and changes to the ring deformation are likely. The shift in the 1097 cm^{-1} peak is also likely due to changes in the ring stretching coordinate, which is the largest contributor to this mode. The disappearance of the 1239 cm^{-1} peak is likely due to the changes to the ring and/or to the $C_5=C_6$ bond strength adjacent to the C_5H and C_6H bonds. The 1388 cm^{-1} band disappearance is clearly due to the fact that the N_3H proton is abstracted. Loss of the 1676 cm^{-1} peak is likely due to the loss of double bond character in $C_4=O$. The new peaks that appear at 1189 , 1290 , 1473 , and 1567 cm^{-1} are likely ring stretches, deformations, and lower frequency carbonyl stretches. The absorption spectra for uracil reveal two absorption bands at different pH values, one attributed to a $(\pi\pi^*)$ transition at $C_5=C_6$ present at pH values below 9 and another band present at higher pH. We attribute this latter band to a $(\pi\pi^*)$ transition from the increased conjugation around N_3 based on the changes to the UVR spectrum.

Conclusions

For both uracil and cytosine, UV resonance Raman spectroscopy shows that an acidic or basic environment not only leads to the simple abstraction or addition of a proton but changes the electron delocalization throughout the molecule. For cytosine, evidence of a change in delocalization is clearly

observed at both pH values below 4 and above 12. At both extremes of pH, the UVRR and absorption spectra predict greater delocalization of the π electrons, throughout the ring at pH values above 12 and centered on N8–C4–C5–C6–N1 at pH values below 4. The lack of sensitivity in uracil's UVRR spectrum to acid indicates that the nitrogens and oxygens are only protonated below pH 1. At basic pH values above 12, the greater electron delocalization observed for uracil is consistent with those observed for cytosine due to deprotonation of N₃.

Acknowledgment. The authors acknowledge support for this research from the NSERC Discovery Grants-in-Aid program.

References and Notes

- (1) Lehninger, A. L. *Biochemistry*; Worth publications: New York, 1975; pp 309–333.
- (2) Saenger, W. *Principles of Nucleic Acid Structure*; Springer-Verlag: New York, 1984; pp 116–133.
- (3) Stimpson, M. M.; Reuter, M. A. *J. Am. Chem. Soc.* **1945**, *67*, 2191–2195.
- (4) Muntean, C. M.; Dostál, L.; Misselwitz, R.; Welfe, H. *J. Raman Spectrosc.* **2005**, *36*, 1047–1051.
- (5) Qin, W.; Zhao, D.; Guo, C. *Chem. Phys. Lett.* **1991**, *184*, 387–390.
- (6) Yarasi, S.; Brost, P.; Loppnow, G. R. *J. Phys. Chem. A* **2007**, *111*, 5130–5135.
- (7) Billingham, B. E.; Yeung, R.; Loppnow, G. R. *J. Phys. Chem. A* **2006**, *110*, 6185–6191.
- (8) Billingham, B. E.; Loppnow, G. R. *J. Phys. Chem. A* **2006**, *110*, 2353–2359.
- (9) Fodor, S. P. A.; Rava, R. P.; Hays, T. R.; Spiro, T. G. *J. Am. Chem. Soc.* **1985**, *107*, 1520–1529.
- (10) (a) Fodor, S. P. A.; Spiro, T. G. *J. Am. Chem. Soc.* **1986**, *108*, 3198–3205. (b) Perno, J. R.; Grygon, C. A.; Spiro, T. G. *J. Phys. Chem.* **1989**, *93*, 5672–5678.
- (11) Kubasek, W. L.; Hudson, B.; Peticolas, W. L. *Proc. Natl. Acad. Sci. U.S.A.* **1985**, *82*, 2369–2373.
- (12) (a) Myers, A. B.; Mathies, R. A. In *Biological Applications of Raman Spectroscopy, Resonance Raman Spectra of Polyenes and Aromatics*; Spiro, T. G. Ed.; Wiley-Interscience: New York, 1987; Vol. 2, pp 1–58. (b) Myers, A. B. Excited Electronic State Properties From Ground-state Resonance Raman Intensities. In *Laser Techniques in Chemistry*; Myers, A. B.; Rizzo, T. R. Eds.; Wiley: New York, 1995; pp 325–384. (c) Kelley, A. M. *J. Phys. Chem. A* **1999**, *103*, 6891–6903.
- (13) Fasman, G. D. Ed. *Handbook of Biochemistry and Molecular Biology, Vol. 1 Nucleic Acids*; Chem. Rubber Co.: Cleveland, OH, 1975; pp 76–206.
- (14) Levene, P. A.; Bass, B. W.; Simms, H. S. *J. Biol. Chem.* **1926**, *70*, 229–241.
- (15) Gaigeot, M. P.; Leulliot, N.; Ghomi, M.; Jobic, H.; Coulombeau, C.; Bouloussa, O. *Chem. Phys.* **2000**, *261*, 217–237.
- (16) Yarasi, S.; Loppnow, G. R. *J. Raman Spectrosc.* **2007**, *38*, 1117–1126.
- (17) Beyere, L.; Arboleda, P.; Monga, V.; Loppnow, G. R. *Can. J. Chem.* **2004**, *82*, 1092–1101.
- (18) Smith, S. O.; Myers, A. B.; Mathies, R. A.; Pardo, J. A.; Winkel, C.; Vandenberg, E. M. M.; Lugtenberg, J. *Biophys. J.* **1985**, *47*, 653–664.

JP811327W